J|A|C|S
ARTICLES
Published on Web 01/10/2006

Organization of Acenes with a Cruciform Assembly Motif

Qian Miao,[†] Xiaoliu Chi,[‡,§] Shengxiong Xiao,[†] Roswitha Zeis,[‡] Michael Lefenfeld,[†] Theo Siegrist,[‡] Michael L. Steigerwald,[†] and Colin Nuckolls*[,†]

Contributions from the Department of Chemistry and The Nanoscience Center, Columbia University, New York, New York 10027 and Bell Laboratories, Lucent Technologies, 600 Mountain Avenue, Murray Hill, New Jersey 07974

Received October 18, 2005; E-mail: cn37@columbia.edu

Abstract: This study explores the assembly in the crystalline state of a class of pentacenes that are substituted along their long edges with aromatic rings forming rigid, cruciform molecules. The crystals were grown from the gas phase, and their structures were compared with DFT-optimized geometries. Both crystallographic and computed structures show that a planar acene core is the exception rather than the rule. In the assembly of these molecules, the phenyl groups block the herringbone motif and further guide the arrangement of the acene core into higher order structures. The packing for the phenyl-substituted derivatives is dictated by close contacts between the C−H's of the pendant aromatic rings and the carbons at the fusions in the acene backbone. Using thiophene substituents instead of phenyls creates cofacially stacked acenes. In thin films, the thiophene-substituted derivative forms devices with good electrical properties: relatively high mobility, high ON/OFF ratios, and low threshold voltage for device activation. An unusual result is obtained for the decaphenyl pentacene when devices are fabricated on its crystalline surface. Although its acene cores are well isolated from each other, this material still exhibits good electrical properties.

Introduction

This study explores the assembly of a class of pentacenes that are substituted along their long edges with aromatic rings forming rigid, cruciform[1] shaped molecules. This work was driven, in part, by curiosity as to how these unusually shaped molecules arrange themselves in the solid state. Despite diphenylpentacene, **2a**, and tetraphenylpentacene, **3**, having been known for over 60 years[2] and even though they have shown promise in light-emitting diodes,[3] their structures in the solid state have not been reported, and very few other derivatives of the phenylated pentacenes have been synthesized.[4,5] Our intention in expanding this class of compounds was to use the sterically encumbered phenyl groups to block the herringbone motif that is typical of many acenes. Given the importance of edge-to-face interactions in π-electron-rich aromatics, we are exploring whether these phenyls could provide a guide to direct the arrangement of the acene core into higher order structures.

Controlling the assembly of linear acenes is an important problem with promise in improving many materials in applications involving intermolecular charge transport.[6] The important finding of this work is that the cruciform acenes have rich diversity in the solid state, including layered, columnar, and cage-like superstructures formed through edge-to-face contacts between the aryl hydrogens and specific atoms in the pentacene backbone. Understanding these assembly characteristics allows the intermolecular contacts to be tuned at the molecular level to adjust the electrical properties.

Results and Discussion

Synthesis. The approach used here successively substitutes the acene core with phenyl rings and studies their structures in the solid state. Figure 1 shows a subset of the phenylated acenes that were synthesized and studied below. **2a** and **3** were synthesized by published procedures,[7] which were adapted to yield the 6,13-di(2′-thienyl)pentacene (**2b**). During the course of this work a paper detailing a preparation of **2b** similar to the present one was reported;[8] compounds **1**, **4**, and **5** (shown below) have not been reported heretofore. **1** was synthesized by addition

[†] Columbia University.
[‡] Bell Laboratories, Lucent Technologies.
[§] Present address: Department of Chemistry, Texas A & M University-Kingsville, MSC 161, 920 W. Santa Gertrudis, Kingsville, TX, 78363.

(1) (a) Klare, J. E.; Tulevski, G. S.; de Picciotto, A.; White, K.; Nuckolls, C. *J. Am. Chem. Soc.* **2003**, *125*, 6030−6031. (b) Klare, J. E.; Tulevski, G. S.; Nuckolls, C. *Langmuir* **2004**, *20*, 10068−10072.
(2) (a) Allen, C. F. H.; Bell, A. *J. Am. Chem. Soc.* **1942**, *64*, 1253−1260. (b) Bendikov, M.; Wudl, F.; Perepichka, D. F. *Chem. Rev.* **2004**, *104*, 4891−4945. (c) Miller, G. P.; Mack, J.; Briggs, J. *Org. Lett.* **2000**, *2*, 3983−3986.
(3) (a) Picciolo, L. C.; Murata, H.; Kafafi, Z. H. *Appl. Phys. Lett.* **2001**, *78*, 2378−2380. (b) Wolak, M. A.; Jang, B.-B.; Palilis, L. C.; Kafafi, Z. H. *J. Phys. Chem. B* **2004**, *108*, 5492−5499.
(4) Miller, G. P.; Briggs, J. *Org. Lett.* **2003**, *5*, 4203−4206.
(5) Duong, H. M.; Bendikov, M.; Steiger, D.; Zhang, Q.; Sonmez, G.; Yamada, J.; Wudl, F. *Org. Lett.* **2003**, *5*, 4433−4436.
(6) (a) Moon, H.; Zeis, R.; Borkent, E.-J.; Besnard, C.; Lovinger, A. J.; Siegrist, T.; Kloc, C.; Bao, Z. *J. Am. Chem. Soc.* **2004**, *126*, 15322−15323. (b) Anthony, J. E.; Brooks, J. S.; Eaton, D. L.; Parkin, S. R. *J. Am. Chem. Soc.* **2001**, *123*, 9482−9483. (c) Payne, M. M.; Parkin, S. R.; Anthony, J. E.; Kuo, C.-C.; Jackson, T. N. *J. Am. Chem. Soc.* **2005**, *127*, 4986−4987. (d) Miao, Q.; Lefenfeld, M.; Nguyen, T.-Q.; Siegrist, T.; Kloc, C.; Nuckolls, C. *Adv. Mater.* **2005**, *17*, 407−412. (e) Swartz, C. R.; Parkin, S. R.; Bullock, J. E.; Anthony, J. E.; Mayer, A. C.; Malliaras, G. G. *Org. Lett.* **2005**, *7*, 3163−3166.
(7) **2a** and **3** were synthesized by phenylation of the corresponding pentacene quinones followed by reduction in acidic conditions, similar to ref 2a.
(8) Vets, N.; Smet, M.; Dehaen, W. *Synlett* **2005**, *2*, 217−222.

10.1021/ja0570786 CCC: $33.50

Scheme 1. Synthesis of Hexaphenyl Pentacene (**4**) and Decaphenyl Pentacene (**5**)

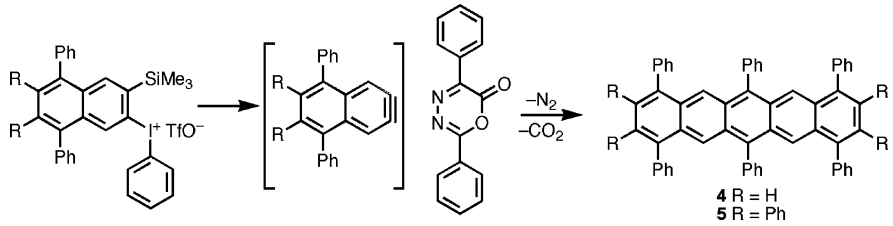

of the appropriate Grignard reagent to the 6-pentacenone followed by dehydration using the procedure of Clar for methyl-substituted pentacene.[9] The synthesis of hexaphenyl and decaphenyl pentacene is shown in Scheme 1. It is similar to one that was developed by Wudl and co-workers to synthesize twistacenes,[3] first generating a naphthyne in situ[10] and trapping it with the diazopyrone.[11] Using this method we have been able to prepare a number of new phenylated pentacenes such as **4** and **5**.

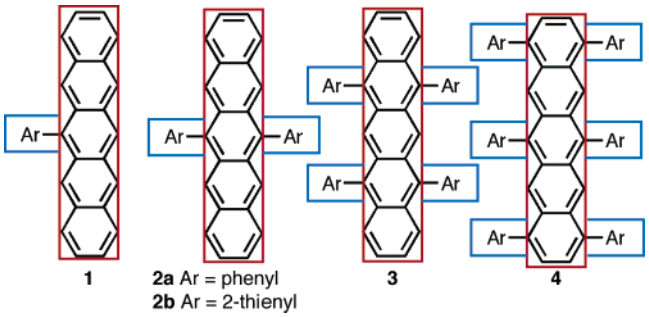

Figure 1. Cruciform π-systems formed from phenylated acenes.

Crystallography. Unsubstituted pentacene is well known to pack into an edge-to-face, herringbone structure. In this structure, the molecules arrange themselves to have C−H bonds of one molecule pointing into a neighboring π face. This is essentially what is expected from the model of Hunter and Sanders for an electron-rich and unsubstituted aromatic ring.[12] There are two metrics of the closeness in these edge-to-face structures. One is the distance between an edge carbon and the aromatic plane, typically around 3.5 Å, and another is the distance between closest intermolecular carbon atoms. In pentacene, close carbon atoms on neighboring molecules are separated by approximately 3.6−3.8 Å.[13]

We grew crystals of the phenyl-substituted aromatics in Figure 1 (**1**−**4**) as well as decaphenylpentacene, **5**.[14] To eliminate complications in the analysis of the crystal structures due to inclusion of solvent, these compounds were grown by vapor transport crystallization.[15] Crystallographic information files and details for the crystal growth for **1**−**5** can be found in the Supporting Information.

The simplest derivative 6-phenylpentacene (**1**) has a "two-faced" molecular structure−−one of its pentacene edges is exposed and available for edge-to-face packing, while the other edge is blocked with a phenyl substituent. The acene structure is slightly twisted out of planarity. Owing to steric interactions with the peri-disposed C−H's in the acene backbone, the pendant phenyl is rotated out of the idealized acene ring plane. The two planes are nearly perpendicular (89.6°). The assembly in the solid state reflects the molecule having "two faces". Both types of intermolecular interactions, edge-to-face contacts between the acene core and π-stacked contacts, are observed in the solid-state assembly. These are indicated with magenta arrows in Figure 2. The cofacial stacking disposes the acene planes approximately 3.5 Å apart (with carbon atoms offset in the familiar honeycomb graphite packing.) The edge-to-face packing is similar to that in pentacene, with the edge carbons pointed at the face of the neighboring acene. The distances between the edge carbons and the neighboring aromatic planes are similar to those observed in the herringbone structure of pentacene.

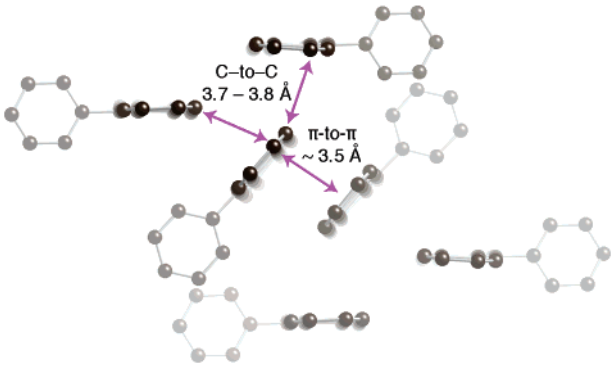

Figure 2. Crystal structure of 6-phenylpentacene, **1**. Magenta arrows show the closest edge-to-face and π-to-π distances. Hydrogens have been removed to clarify the view.

To contrast the isolated molecular structure with that observed in the crystal, we conducted density functional theory (DFT)[16] simulations. The optimized molecular geometry of **1** differs from what we observe in the crystal in two subtle ways: the acene unit is essentially planar, and the angle between this plane and the plane of the phenyl ring is noticeably smaller (81° vs 89.6°).

(9) Clar, E. *Chem. Ber.* **1949**, *82*, 495−514.
(10) Using the procedure of Kitamura, T.; Yamane, M.; Inoue, K.; Todaka, M.; Fukatsu, N.; Meng, Z.; Fujiwara, Y. *J. Am. Chem. Soc.* **1999**, *121*, 11674−11679.
(11) (a) Steglich, W.; Buschmann, E.; Gansen, G.; Wilschowitz, L. *Synthesis* **1977**, *4*, 252−253. (b) Farina, C.; Pifferi, G.; Nasi, F.; Pinza, M. *J. Heteroat. Chem.* **1983**, *20*, 979−982.
(12) Hunter, C. A.; Sanders, J. K. M. *J. Am. Chem. Soc.* **1990**, *112*, 5525−5534.
(13) (a) Campbell, R. B.; Robertson, J. M. *Acta Crystallogr.* **1962**, *15*, 289−290. (b) Holmes, D.; Kumaraswamy, S.; Matzger, A. J.; Vollhardt, K. P. C. *Chem. Eur. J.* **1999**, *5*, 3399−3412. (c) Siegrist, T.; Kloc, C.; Schön, J. H.; Batlogg, B.; Haddon, R. C.; Berg, S.; Thomas, G. A. *Angew. Chem., Int. Ed.* **2001**, *40*, 1732−1736. (d) Mattheus, C. C.; Dros, A. B.; Baas, J.; Meetsma, A.; de Boer, J. L.; Palstra, T. T. M. *Acta Crystallogr., Sect. C.* **2001**, *57*, 939−941.
(14) The crystallographic information files for **1**−**5** are available in the Supporting Information.
(15) All the crystals were grown by vapor transport crystallization except that of 6-phenylpentacene (**1**), which was grown by sublimation under vacuum. See Supporting Information for preparation of the crystals. For vapor transport crystallization, see: Laudise, R. A.; Kloc, C.; Simpkins, P. G.; Siegrist, T. *J. Cryst. Growth* **1998**, *187*, 449−454.
(16) All density functional theory calculations were performed using Jaguar 6.0, Schrödinger, L.L.C., Portland OR, 1991−2004. The geometries were optimized in each case assuming no a priori molecular symmetry. The calculations used the B3LYP hybrid functional and 6-31G** basis sets throughout. Calculated molecular geometries for **1**−**5** can be found in the Supporting Information.

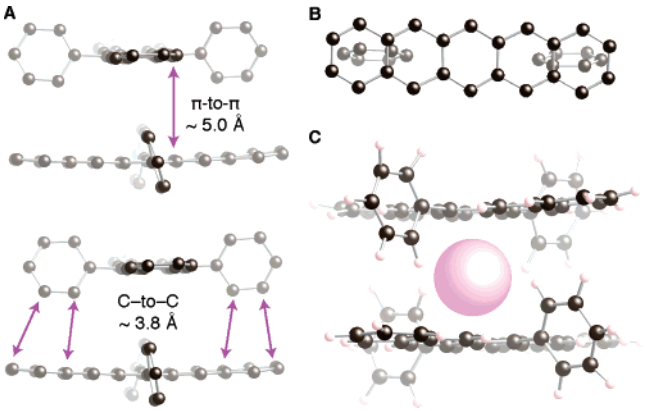

Figure 3. Crystal structure of 6,13-diphenylpentacene, **2a**, showing (A) infinite columns of cage-like superstructures (hydrogens have been removed to clarify the view) and (B) assembly motif where the edges of the phenyls point at the acene core. (C) The magenta sphere shows the small volume of unused space between the acenes.

Further substitution to give 6,13-diphenylpentacene (**2a**) blocks the assembly that was seen in 6-phenylpentacene. The crystal structure, Figure 3, shows that the acene cores are arranged cofacially but the long axes of nearest neighboring acenes are orthogonal, resulting in a cage-like superstructure. The acene core is bowed along its long axis; this can be seen clearly in Figure 3A. Figure 3B shows the (phenyl)edge-to-(acene)face interactions that are responsible for the assembly. The angle between the ideal acene plane and either of the phenyl planes is 76°. This twist in the aryl rings of **2a** directs them at the neighboring acene core. Specifically, the carbons at the fusion points between the terminal rings and end rings are the ones that are close (approximately 3.8 Å from carbon to carbon). Infinite columns of these cage-like structures are packed into a square lattice.

Again, in order to gain insight into crystal-packing forces, we conducted DFT simulations on the isolated molecule. These calculations show small disagreements with the crystal structure: there is a slight longitudinal twist, as opposed to the observed bowing, in the acene 'plane', and the angle between the acene plane and either of the phenyl rings is 80°. These variations are energetically negligible, and they hint at the flexibility of the acene. It is interesting to note that DFT simulations show that the observed, 'staggered' arrangement of the two phenyl rings is energetically degenerate with the 'eclipsed' arrangement.

What is remarkable about the assembly motif of **2a** is that the acenes are well outside their van der Waals distance from each other; the aromatic planes of the pentacene are approximately 5.0 Å apart. This creates a volume of open space inside the cage structure shown in Figure 3C that could accommodate the smallest of guests, for example, dihydrogen. It may also be possible to extend this motif to make more capacious interiors by substituting the 6,13-phenyl substituent groups with longer acenes such as anthracene or pentacene itself.

The tetraphenyl pentacene **3** is the only derivative prepared for this series not having substituents at the 6- and 13-positions and may be considered a close relative to rubrene. The phenyl side chains are twisted to near perpendicular (~90°) with respect to the acene core. The pentacene backbone is essentially flat. The core lacks the contortions that were observed for the mono- and diphenyl derivatives. In this case, again, edge-to-face interactions dominate the structure. The crystal packing is

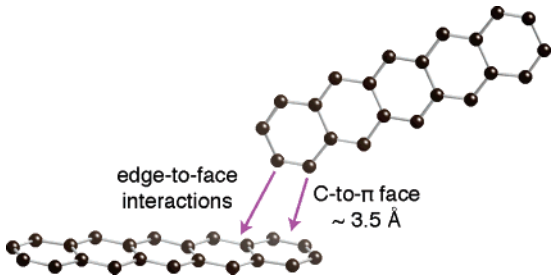

Figure 4. Crystal structure of tetraphenyl pentacene, **3**. Phenyl side chains and the hydrogens have been suppressed in this view. The magenta arrows show close contacts between the edge of one acene and the face of another.

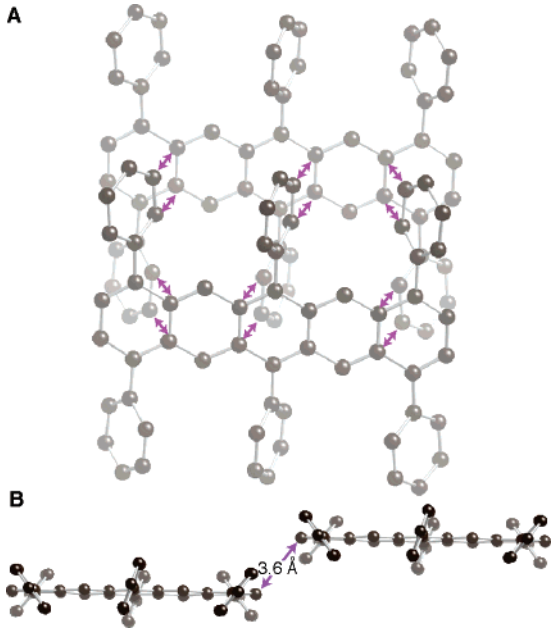

Figure 5. Crystal structure of hexaphenyl pentacene, **4**: (A) magenta arrows showing the 12 close contacts (approximately 3.8 Å C-to-C) between the phenyl side chains and the acene core; (B) 3.6 Å separates the ends of the acenes (shown with a magenta arrow). Hydrogens have been removed to clarify the view.

visually complex and difficult to parse. Shown in Figure 4 are two of the acenes from the crystal structure with the rest of the molecular structure (i.e., the hydrogens and pendant phenyls) suppressed. The acene cores daisy chain together along the long axis of the acene by poking one edge of its termini into the face of a neighboring aromatic plane. DFT simulations on the isolated molecule show a planar acene core with phenyl−acene dihedral angles of 79°, 81°, 86°, and 90°. There is essentially no bending of the phenyl rings away from one another−−in other words, in each phenyl, the C1−C4 vector is perpendicular to the long axis of the acene.

As the acene core becomes more substituted the side chains begin to dictate the types of edge-to-face interactions. In hexaphenyl pentacene, **4**, we see an extreme case of this where the phenyls direct the supramolecular assembly (Figure 5). This material forms a layered structure in which each layer is interlocked with its neighbors by the molecular corrugation provided by the pendant phenyl substituents. Between two neighbors there are 12 contacts, the phenyl side chains of one molecule pointing "sideways" at the acene fusion carbons of the other (these are highlighted in Figure 5a with magenta arrows). In each molecule the two central phenyls are reclined to around 70° with respect to the acene core, and they are

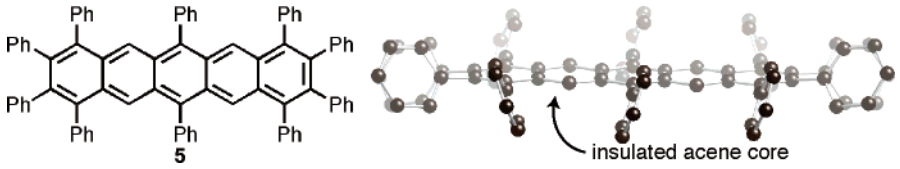

Figure 6. Molecular structure and crystal structure of decaphenylpentacene (**5**). The phenyl side chains form a "picket fence" around the acene core.

eclipsed with respect to each other. Each of the outer phenyls, colliding with only a single peri CH group, is able to relax to an angle of approximately 50° with respect to the acene and is staggered with respect to its cross-acene relative. The acene backbone is twisted slightly along its long axis. The ends of the acenes form edge-to-face interactions between neighboring terphenyl subunits. This holds the acenes relatively close to each other (~3.6 Å), shown in the magenta arrows in Figure 5B. DFT simulations agree quite well with the crystallographically determined molecular structure: there is a distinct twist in the acene, the central phenyls are eclipsed and at an angle of 72−75° with respect to the acene, and the outer phenyls are mutually staggered at angles of 50−55° to the acene.

Compound **5** (shown in Figure 6), the most highly substituted derivative prepared here, has 10 phenyls attached to its core. This compound has many similarities in packing and structure to the hexaphenyl pentacene, **4**. The structure of the subunits again has the central phenyl substituents eclipsed while the outer ones adopt an anti-conformation. The intermolecular packing is also similar to the contacts seen for the hexaphenyl pentacene. The primary difference in the packing is that the close contact between the ends of the pentacene cores that is seen for **4** (shown in Figure 5B) is not possible for **5** with each pentacene being greater than 5.1 Å away from each other. The phenyl side chains form a picket fence around the acene core and insulate any close contact between the acene cores.

Several generalities about the packing of the acenes can be drawn from the crystal structures of this series. One is that distorting the acene core from planarity is common. This is a reflection of the fact that as one goes higher in the acene series, the effect of 'aromatization' decreases. Another generalization is that the central diphenyls tend to be eclipsed. Since our DFT simulations detect no significant energetic difference between the eclipsed and staggered conformers, we conclude that this is due to more efficient crystal packing in the eclipsed form. The underlying assembly motif that is found to be pervasive for this class of cruciform π systems can be seen in the crystal structure of **2a**. Each of the other compounds crystallized for this study−−the tetraphenyl pentacene (**3**),[17] hexaphenyl pentacene (**4**), and decaphenylpentacene (**5**)−−shows close contacts between aryl C−H groups and the fusion points along the acene backbone.

Because the edge-to-face interactions between the phenyl side chains and the acene core were so common for these cruciform acenes, we became interested to see how the molecular assembly would respond if the phenyls were substituted with thiophenes. In each pendant group this substitution replaces two aryl carbon hydrogen bonds with a single sulfur lone pair. The crystal structure of the 6,13-di(2′-thienyl)pentacene, **2b**, is shown in Figure 7. The acene has a very slight twist along its long axis, similar to its phenyl counterpart **2a**. The thiophene planes are essentially perpendicular to the acene core. The sulfur atoms

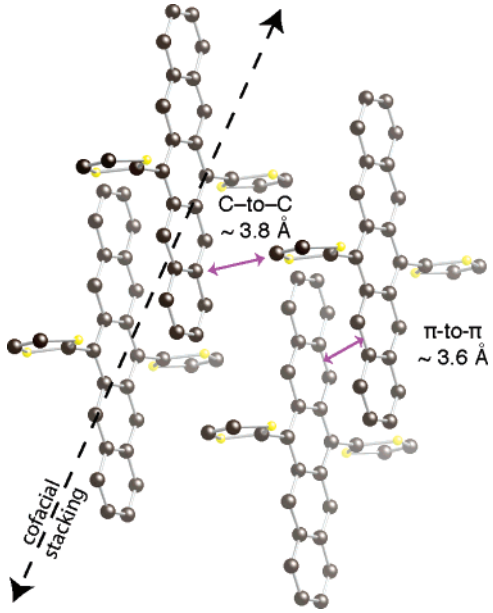

Figure 7. Crystal structure of 6,13-di(2′-thienyl)pentacene, **2b**, showing a cofacial, one-dimensional stack. The magenta arrows show the close contacts between the acene faces and neighboring columns. The position of the sulfur atoms (yellow balls) is disordered in the crystal.

are disordered in the crystal structure. DFT simulations aid in understanding this disorder. As might be expected, we found two locally stable geometries for **2b**, one having the thiophenes rotated such that the S atoms are on the same side of the acene (syn) and the other having the S atoms on opposite sides (anti). The two forms are energetically degenerate to within the limit of our calculations; however, the geometries of the two forms differ significantly. In the anti form there is a twist in the acene along its long axis. This is similar to the twist seen in the crystal structures of **1** and **4** as well as **2b**. In the syn form, on the other hand, the acene is not twisted but rather it is bowed significantly. In this way this structure is similar to that observed crystallographically in **2a**. We suggest that the observed disorder in the present structure is due to a random mixture of the two rotamers in the single crystal.

The cores, with little other option, stack into a cofacial arrangement with a honeycomb, graphite packing. The aromatic planes are close packed with planes being ~3.6 Å apart from each other. This structure is similar to the structure obtained by Anthony and co-workers for the 6,13-diethynyl-substituted pentacene.[18] The contact between adjacent, co-facial stacks is from the 3-position of the thiophene to the carbons at the fusion points on the neighboring acene faces, shown in Figure 7.

Electrical Measurements in Thin Films. The pentacene derivatives were prepared because they could have utility in electronic and optoelectronic applications such as field effect transistors and light-emitting diodes. Each of these materials (**1**−**5**) was tested as the semiconductor in field effect transistors

(17) See Supporting Information for the crystal structure of the tetraphenyl pentacene **3**.

(18) See ref 6b.

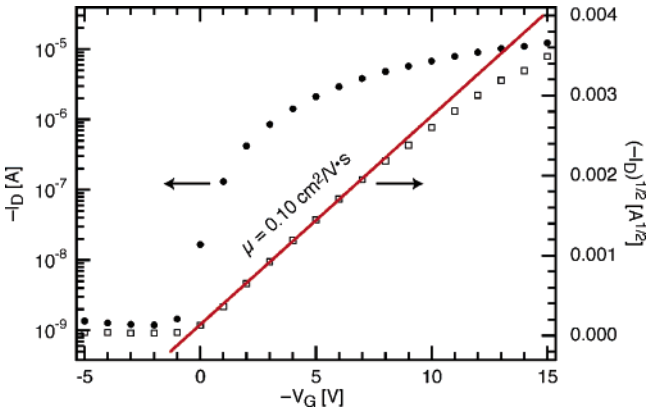

Figure 8. Gate voltage versus the drain current for a thin film transistor of **2b** on OTS-treated SiO_2 (100 nm thick) with $W = 2$ mm, $L = 45$ μm, $C_i = 30$ nF/cm^2. The red line is a curve fit through the linear portion of the curve. The source drain bias voltage is held at −20 V.

Table 1. Field Effect Mobility in Thin Film Transistors of Cruciform-Shaped Pentacenes[19]

	field effect mobility (cm²/V·s)
1	2×10^{-4}
2a	8×10^{-5}
2b	0.10
3	1×10^{-3}
4	4×10^{-4}
5	no FET

fabricated from thin films on silicon substrates or directly on the surface of their crystals. Perhaps it is not surprising, given that pentacene is such a workhorse in thin film organic electronics, that all of these materials behave as p-type, hole-transporting semiconductors.

In thin film transistors, their field effect mobilities are summarized in Table 1. The trend is what one would guess from the crystal packing detailed above. The structures that have the acenes isolated from each other, like the diphenyl pentacene (**2a**) and the decaphenylpentacene (**5**), have poor transistor characteristics. Structures that allow the acenes to touch, such as tetraphenyl pentacene, **3**, and hexaphenyl pentacene, **4**, but have qualitatively and quantitatively poor π overlap have intermediate mobilities values.

2b, which has the best π overlap of this series, shows very good electrical properties.[20] With very little optimization[21] the mobility of **2b** was found to be approximately 0.1 cm^2/V·s in thin film devices. Shown in Figure 8 are typical data for the drain current as a function of the gate bias voltage. Here we use measured values for the capacitance of the gate dielectric layer. For an OTS-treated 100 nm SiO_2 layer the capacitance was 30 nF/cm^2. For an OTS-treated 300 nm SiO_2 layer the capacitance was 11.3 nF/cm^2. If more conventional values were used, the mobility in these devices would be considerably higher (~5−10 times higher). The transistors switch on sharply and yield a low threshold voltage (~0 V). The ON/OFF ratio (measured from $V_G = 1$ to −15 V) is 10^4. With a thicker oxide layer (300 nm) and higher gate voltage (−100 V) the ON/OFF

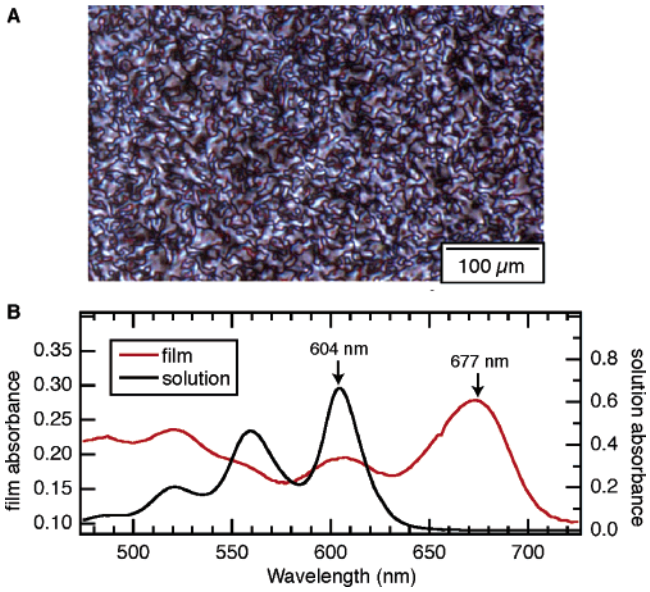

Figure 9. (A) Polarized micrograph of a thermally evaporated film of **2b** (40 nm thick) deposited on a glass plate. The substrate was held at ~80 °C during deposition. (B) UV−vis spectra comparing a 100 nm thick film of **2b** thermally evaporated onto a quartz slide held at ~80 °C during deposition and a solution (70 μm in CH_2Cl_2, path length = 1 cm).

ratio (measured from $V_G = 0$ to −100 V) for **2b** rises to 10^6. Moreover, we have done very little to optimize these values and they represent a lower limit on what could be expected for the intrinsic mobility in **2b**.

Figure 9A shows a polarized light micrograph of one of the films of **2b** deposited onto a glass surface that was held at 80 °C. Between crossed polarizers the film has the appearance of dark threads running throughout the birefringent film reminiscent of the textures observed in nematic liquid crystals. This material represents a conundrum. Even though this material has the textures shown in Figure 9A indicative of anisotropy, no surface X-ray scattering peaks were observed over a broad range of *d* spacings. Despite the lack of long-range organization of this material, it does exhibit a significant amount of π stacking, based on its UV−vis spectra. Figure 9B compares the long wavelength spectra from a dilute CH_2Cl_2 solution (7×10^{-5} M) and from a 100 nm thick film on quartz. The longest wavelength absorbance for **2b** shifts to the red by approximately 73 nm on going from solution (604 nm) to a thin film (677 nm). We attribute this shift to the delocalization of the excited state due to π stacking. Red shifts of this type are common in many π-stacked systems.[22] Bringing together thin film microscopy, spectroscopy, and X-ray diffraction with the crystal structure shown in Figure 7 it is possible to construct a model of how the material organizes in thin films. We assume that the material organizes into the π-stacked columns and that there is only a loose correlation between neighboring columns. This may explain the lack of long-range order while retaining the good electrical properties.

It is remarkable that despite the lack of obvious long-range order these films still show good electrical properties. It is

(19) **2a** was deposited on bare SiO_2. The others were deposited on octadecyl trichlorosilane (OTS) treated SiO_2. See ref 6d for the OTS substrate preparation.
(20) The mobility is calculated by plotting $|I_{DS}|^{1/2}$ against $|V_G|$ and using the equation $I_{DS} = (mC_iW/2L)(V_G - V_0)^2$.
(21) The mobility of 0.1 cm^2/V·s is achieved when **2b** was evaporated onto octadecyltrichlorosilane (OTS) treated SiO_2 (100 nm)/Si substrate held at 80 °C.
(22) (a) Nguyen, T.-Q.; Martel, R.; Avouris, P.; Bushey, M. L.; Brus, L.; Nuckolls, C. *J. Am. Chem. Soc.* **2004**, *126*, 5234−5242. (b) Braitbart, O.; Sasson, R.; Weinreb, A. *Mol. Cryst. Liq. Cryst.* **1988**, *159*, 233−242. (c) Nuckolls, C.; Katz, T. J.; Castellanos, L. *J. Am. Chem. Soc.* **1996**, *118*, 3767−3768. (d) Rohr, U.; Schilichting, P.; Böhm, A.; Gross, M.; Meerholz, K.; Bräuchle, C.; Müllen, K. *Angew. Chem., Int. Ed.* **1998**, *37*, 1434−1437. (e) Xiao, S.; Myers, M.; Miao, Q.; Sanaur, S.; Pang, K.; Steigerwald, M. L.; Nuckolls, C. *Angew. Chem.* **2005**, *44*, 7390−7394.

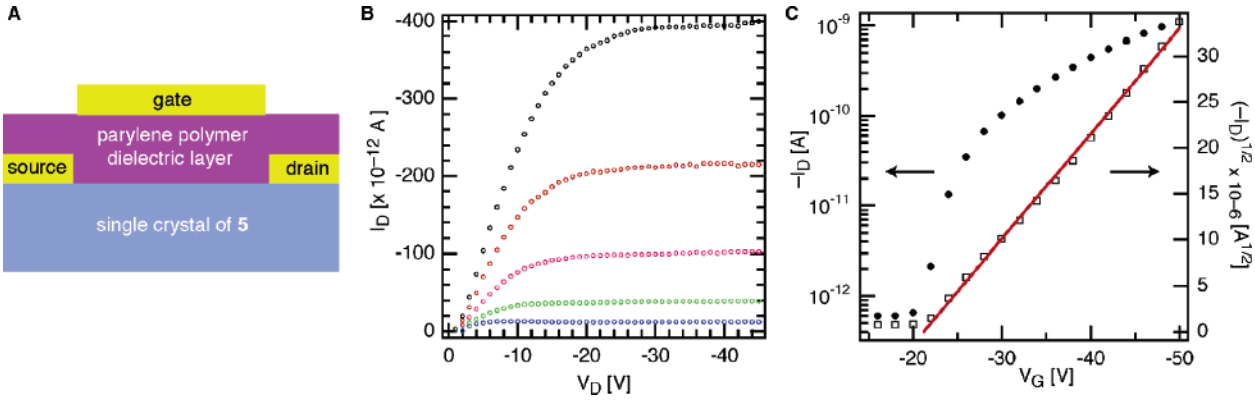

Figure 10. (A) Schematic of the devices fabricated on the crystals of **5**. (B) Transistor output curves with a gate bias from −20 (blue curve) to −40 V (black curve) in 5 V steps. (C) Gate voltage versus the drain current. The red line is a curve fit through the linear portion of the curve. The source drain bias voltage was −60 V.

known that the field effect mobility is very sensitive to the crystallinity of the thin films.[23] For example, an amorphous pentacene film has a mobility of 10^{-9} $cm^2/V\cdot s$, while a highly ordered film of pentacene on the same substrate shows a mobility of around 0.6 $cm^2/V\cdot s$.[2b,23] The hole mobilities measured using time-of-flight methods for amorphous organic semiconductors are much lower, typically in the range from 10^{-4} to 10^{-3} $cm^2/V\cdot s$.[24] **2b** may find utility in various applications where amorphous films can be advantageous.[23]

Electrical Measurements on Crystals. As a point of comparison and to begin the process of determining the intrinsic mobilities of these materials, we measured the electrical properties in devices constructed on the surface of the crystals.[24,25] The obstacles to preparing devices on these crystals were that the quality of the crystals was not high and the crystals were in general small. The decaphenyl pentacene **5** grew into relatively large crystallites that had a milky appearance. The process for device fabrication is shown in Figure 10A and has been described elsewhere.[25]

We expected that **5** would be inactive in crystalline devices because its acene cores are held apart by such a great distance and because its thin film devices were inactive. To our surprise, **5** behaves like a hole-transporting semiconductor. Current−voltage curves showing the transistor output and gate sweep are shown in Figure 10B,C. The mobility in these materials is 1.4×10^{-3} $cm^2/V\cdot s$. The device switches on sharply but at high gate bias. The high threshold indicates charge trapping, which could reflect the interface between and the crystal and the parylene dielectric layer to be of a low quality. Given how isolated the acene core is from its nearest neighbors it is difficult to conceive the path for the charge carriers in this material. Either the charge must move from the acene core into the phenyl side chain or it must take an extremely long hop to a neighboring acene core. Either way, it is remarkable that a material with its acene cores separated well outside their van der Waals radius are able to exhibit charge transport.

Conclusions

This study describes the molecular structures, crystal structures, and electrical properties for acenes that are substituted with aryl side chains. In many of these derivatives the acene cores deviate from planarity. The packing for the phenyl-substituted derivatives is dictated by close contacts between the C−H's of the pendant aromatic rings and the carbons at the fusions in the acene backbone. Thiophenes block this mode of packing and yield cofacially stacked acenes. Each of these derivatives was evaluated in thin film transistors and transistors constructed on the surface of single crystals. In thin films the thiophene-substituted derivative (**2b**) forms devices with good electrical properties: relatively high mobility, high ON/OFF ratios, and low threshold voltage for the devices to turn on. An unusual result is obtained for the decaphenyl pentacene when devices are fabricated on its crystalline surface. Although its acene cores are well isolated from each other, the material still exhibits good electrical properties. This highlights how important it will be to evaluate these and other organic semiconductors in single-crystal devices given the limited number of structures that have been tested in this manner.[26]

Acknowledgment. We acknowledge primary financial support from the Nanoscale Science and Engineering Initiative of the National Science Foundation under NSF Award Number CHE-0117752 and by the New York State Office of Science, Technology, and Academic Research (NYSTAR) and the Department of Energy, Nanoscience Initiative (NSET#04ER46118). C.N. thanks the National Science Foundation CAREER award (#DMR-02-37860), the American Chemical Society PRF type G (#39263-G7), the Camille Dreyfus Teacher Scholar Program (2004), and the Alfred P. Sloan Fellowship Program (2004). We thank the MRSEC Program of the National Science Foundation under Award Number DMR-0213574 and the New York State Office of Science, Technology, and Academic Research (NYSTAR) for financial support for M.L.S. and the shared instrument facility.

Supporting Information Available: Details for the preparation and characterization of **1**−**5**, crystallographic information files (**1**−**5**), optimized DFT geometries (**1**−**4**), and device preparation for **1**−**5**. See any current masthead page for ordering information and Web access instructions.

JA0570786

(23) Dimitrakopoulos, C. D.; Malenfant, P. R. L. *Adv. Mater.* **2002**, *14*, 99−117.
(24) Grazulevicius, J. V.; Strohriegl, P. *Adv. Mater.* **2002**, *14*, 1439−1452.
(25) Butko, V. Y.; Chi, X.; Lang, D. V.; Ramirez, A. P. *Appl. Phys. Lett.* **2003**, *83*, 4773−4775.
(26) (a) See ref 25. (b) Menard, E.; Podzorov, V.; Hur, S.-H.; Gaur, A.; Gershenson, M. E.; Rogers, J. A. *Adv. Mater.* **2004**, *16*, 2097−2101. (c) Sundar, V. C.; Zaumseil, J.; Podzorov, V.; Menard, E.; Willett, R. L.; Someya, T.; Gershenson, M. E.; Rogers, J. A. *Science* **2004**, *303*, 1644−1647. (d) Butko, V. Y.; Chi, X.; Ramirez, A. P. *Solid State Commun.* **2003**, *128*, 431−434.